Lyapunov based control of hybrid energy storage system in electric vehicles

El Fadil, H.; Giri, F.; Guerrero, Josep M.

Published in:
Proceedings of the American Control Conference (ACC), 2012

Publication date:
2012

Document Version
Early version, also known as pre-print

This document is a preprint of the final paper: *El Fadil, H.; Giri, F.; Guerrero, J.; , "Lyapunov based control of hybrid energy storage system in electric vehicles," American Control Conference (ACC), 2012 , vol., no., pp.5005-5010, 27-29 June 2012*
URL: http://ieeexplore.ieee.org/stamp/stamp.jsp?tp=&arnumber=6314673&isnumber=6314593

Lyapunov Based Control of Hybrid Energy Storage System in Electric Vehicles

H. El Fadil, F. Giri, Josep M. Guerrero

***Abstract*—This paper deals with a Lyapunov based control principle in a hybrid energy storage system for electric vehicle. The storage system consists on fuel cell (FC) as a main power source and a supercapacitor (SC) as an auxiliary power source. The power stage of energy conversion consists on a boost converter connected with the main source and a buck-boost converter connected with the auxiliary source. The converters share the same dc bus which is connected to the traction motor through an inverter. The aim is controlling power converters in order to satisfy the following requirements: i) tight dc bus voltage regulations, ii) perfect tracking of SC current to its reference, and iii) asymptotic stability of the closed loop system. It is clearly shown, using formal analysis and simulations that the designed controller meets all the objectives.**

I. Introduction

Oil crisis and environmental issues continue to worry vehicle manufacturers. Nowadays, much research has been undertaken on technologies for future vehicles. Among these technologies the hybrid electric vehicle (HEV) is an efficient and promising solution ([1], [2]).

Most hybrid electric vehicle configurations use two energy storage devices: one with high energy storage capability, called "Main Energy System" (MES), and the other with high power capability and reversibility, called "Auxiliary Energy System" (AES). The MES provides extended driving range and the AES good acceleration and regenerative braking.

Accordingly, Fuel cell (FC) based vehicles have the potential to improve significantly the fuel economy and can be more efficient than traditional internal combustion engines ([3], [4], [5]). The development and infrastructure of FC technologies have been advancing rapidly to improve overall system efficiency under realistic automotive loads while meeting the demands for dynamic response under transient loads or cold start conditions ([6], [7]. Although there are various FC technologies available for use in vehicular systems, according to scientists and vehicle developers, a prime candidate is the proton exchange membrane FC (PEMFC), [8], because the PEMFC has higher power density and lower operating temperatures than other types of FC systems.

A stand alone FC system integrated into an automotive power train is not always sufficient to provide the load demands of a vehicle [9]. To provide the initial peak power during transients such as start up, acceleration or sudden changes in load and also to take advantage of the regenerative power of an electric vehicle at braking, a supercapacitor (SC) bank is needed in addition to the FC ([10], [11], [8]).

To ensure the dynamic exchange of energy between the FC source, the load and the SC modules, various converter topologies and their control are presented ([12], [13]). The general system topology is represented in Fig. 1 which is usually called hybrid energy storage system (HESS).

The control of the HESS has been studied by using conventional linear control techniques (see e.g. [14], [15], [16], [17], [18], [19]). However both the dc-dc converters and the fuel cell exhibit a highly nonlinear behavior [20], so that linear control only can ensure stability for a certain operation point. In this paper the modeling and the nonlinear control strategy for a hybrid energy storage system is investigated.

The paper is organized as follows: in Section 2, the HESS in electric vehicle is described; Sections 3 is devoted to the system modeling; controller design and closed-loop analysis is presented in Section 4; the controller performances are illustrated by numerical simulation in Section 5; Section 6 provides a conclusion of the paper.

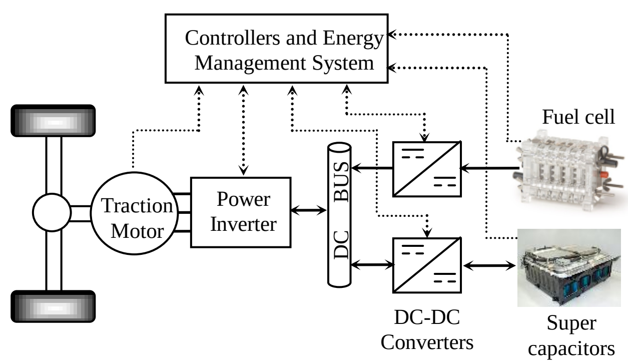

Fig.1: Power circuit of typical hybrid vehicle

II. Presentation Of Electric Circuit Structure

Figure 2 shows the studied hybrid energy storage system (HESS) of the electric vehicle. It consists of a 400-V dc link supplied by a 27kW PEMFC used as the main source, through a current nonreversible dc/dc converter, a SC bank used as an auxiliary source and which is connected to the dc link through a current reversible dc/dc converter, and the load represented by the inverter driving the electric motor.

The function of the FC is to supply mean power to the load,

Manuscript received September, 2011.
H. El Fadil is with the ENSA, Ibn Tofail University, Kénitra, Morocco, (e-mail: el_fadil_hassan@univ-ibntofail.ac.ma, corresponding author).
F. Giri is with the GREYC Lab, UMR CNRS, University of Caen, 14032, Caen, France (e-mail: giri@greyc.ensicaen.fr).
J.M. Guerrero is with the Aalborg University, Denmark (e-mail: josep.m.guerrero@upc.edu, joz@et.aau.dk).

whereas the SC is used as a power source: it supplies transient power demand, and peak loads required during acceleration and deceleration.

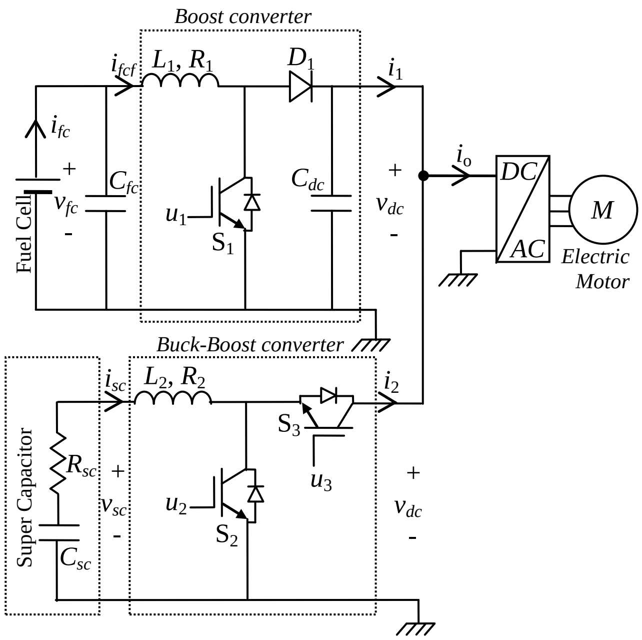

Fig.2: Fuel cell supercapacitor hybrid energy storage system

A. FC converter (boost)

As the main source FC is not current reversible the boost power is used to adapt the low dc voltage delivered by the FC at rated power of dc bus [14]. Thus, it is composed of a high frequency inductor L_1, an output filtering capacitor C_{dc}, a diode D_1 and a main switch, insulated-gate bipolar transistor (IGBT), S_1 controlled by a binary input signal u_1. The input capacitor C_{fc} is used to protect the FC against overvoltage in transient high power demand of the load.

B. SC converter (buck-boost)

The SC is connected to the dc bus by means of a two-quadrant dc/dc converter, also called buck-boost converter. Supercapacitor current, which flows across the storage device, can be positive or negative, allowing energy to be transferred in both directions. L_2 represents the inductor used for energy transfer and filtering. The inductor size is classically defined by switching frequency and current ripple [21]. The converter is driven by means of binary input signals u_2 and u_3 applied on the gates of the two IGBTs S_2 and S_3, respectively.

C. Energy management strategy of hybrid power source

The main energy management strategy for the combined system reported in many places ([21], [22], [23], [24]).
To realize the energy-management strategy the dc-dc power converters has to be properly controlled. Accordingly, the boost converter is driven to realize a classical dc bus voltage regulation. The buck-boost converter is driven so that the SC current i_{sc} perfectly tracks its reference I_{scref} which is generated by the energy management system. The generation of current reference I_{scref} is not treated in this work as the focus is made on the power converters non linear controller design. However, this current is positive in discharging mode and negative in charging mode [14].

III. Hybrid Energy Storage System Modeling

A. Energy sources models

The classical static V-I polarization for a fuel cell is known to be nonlinear [25]. The voltage reduction is caused by three major losses: activation losses, ohmic losses, and transport losses.
The Supercapacitor can be represented by its classical equivalent circuit consisting of a capacitance (C_{sc}), an equivalent series resistance (ESR, R_{sc}) representing the charging and discharging resistance and an equivalent parallel resistance (EPR) representing the self discharging losses ([26], [27]).

B. Boost converter modeling

From Fig. 2 one can obtain the power stage bilinear equations, considering some non-idealities. For instance, the inductances L_1 and L_2 shown in Fig.2 present an equivalent series resistance (ESR), R_1 and R_2, respectively. Each IGBT switch is controlled by using a PWM signal u_j (j=1,2,3) which takes values from the subset {0, 1}.
From inspection of the circuit, shown in Fig.2, and taking into account that u_1 can take the binary values 1 or 0, the following bilinear switching model can be obtained:

$$\frac{di_{fcf}}{dt} = -(1-u_1)\frac{v_{dc}}{L_1} - \frac{R_1}{L_1} i_{fcf} + \frac{v_{fc}}{L_1} \tag{1a}$$

$$\frac{dv_{dc}}{dt} = (1-u_1)\frac{i_{fcf}}{C_{dc}} - \frac{1}{C_{dc}} i_1 \tag{1b}$$

where i_{fcf} and i_1 being, respectively, the inductor input current and the output current of the boost converter; v_{fc} the FC voltage; v_{dc} the dc bus voltage.

C. Buck-Boost converter modeling

This converter can operate as a boost converter or a buck converter. Indeed, in discharging mode of the SC ($i_{sc} > 0$) the converter operates as a boost converter, however, in charging mode of SC ($i_{sc} < 0$) it operates as a buck converter. As our goal is to enforce the SC current i_{sc} to track its reference i_{scref} provided by the energy management system, one can define a binary variable k as follows:

$$k = \begin{cases} 1 \quad if \quad i_{scref} > 0 \quad \text{(Boost mode)} \\ 0 \quad if \quad i_{scref} < 0 \quad \text{(Buck mode)} \end{cases} \tag{2}$$

1) Boost mode operation (k=1)

In this case the control input signal u_3 is fixed to zero (u_3=0) and u_2 is a PWM variable input. From inspection of the circuit, shown in Fig.2, and taking into account that u_2 can take the binary values 1 or 0, the following bilinear switching model can be obtained:

$$\frac{di_{sc}}{dt}=-(1-u_2)\frac{v_{dc}}{L_2}-\frac{R_2}{L_2}i_{sc}+\frac{v_{sc}}{L_2} \tag{3a}$$

$$i_2=(1-u_2)i_{sc} \tag{3b}$$

where i_{sc} being the SC current.

2) Buck mode (k=0)

The control input signal u_2 is fixed to zero (u_2=0) and u_3 acts as the PWM variable input. Also, from Fig. 2, and tacking in account that $u_3 \in \{0,\ 1\}$, the following model can be obtained

$$\frac{di_{sc}}{dt}=-u_3\frac{v_{dc}}{L_2}-\frac{R_2}{L_2}i_{sc}+\frac{v_{sc}}{L_2} \tag{4a}$$

$$i_2=u_3 i_{sc} \tag{4b}$$

D. Global system model

On the basis of the previous three partial models ((1), (3) and (4)), the aim now is to obtain a global model of the system useful for control design purpose. From the inspection of (3) and (4) one can ready obtain the following buck boost converter global model:

$$\frac{di_{sc}}{dt}=-\left[k(1-u_2)+(1-k)u_3\right]\frac{v_{dc}}{L_2}-\frac{R_2}{L_2}i_{sc}+\frac{v_{sc}}{L_2} \tag{5a}$$

$$i_2=\left[k(1-u_2)+(1-k)u_3\right]i_{sc} \tag{5b}$$

In the other hand, from Fig.2 and taking into account (5b) one obtains:

$$i_1=i_o-i_2=i_o-\left[k(1-u_2)+(1-k)u_3\right]i_{sc} \tag{6}$$

where i_o being the load current.

Finally, using ((1), (5a) and (6) the following bilinear switched model of the global system is obtained:

$$\frac{di_{fcf}}{dt}=-(1-u_1)\frac{v_{dc}}{L_1}-\frac{R_1}{L_1}i_{fcf}+\frac{v_{fc}}{L_1} \tag{7a}$$

$$\frac{di_{sc}}{dt}=-u_{23}\frac{v_{dc}}{L_2}-\frac{R_2}{L_2}i_{sc}+\frac{v_{sc}}{L_2} \tag{7b}$$

$$\frac{dv_{dc}}{dt}=(1-u_1)\frac{i_{fcf}}{C_{dc}}+u_{23}\frac{i_{sc}}{C_{dc}}-\frac{i_o}{C_{dc}} \tag{7c}$$

Where u_{23} is the only control input variable of the buck-boost converter defined as follows:

$$u_{23}=k(1-u_2)+(1-k)u_3 \tag{8}$$

The generation of effective control input signals u_2 and u_3 from u_{23} will be investigated later in this paper.

For control design purpose, it is more convenient to consider the following averaged model, obtained by averaging the model (7) over one switching period

$$\frac{dx_1}{dt}=-(1-\mu_1)\frac{x_3}{L_1}-\frac{R_1}{L_1}x_1+\frac{v_{fc}}{L_1} \tag{9a}$$

$$\frac{dx_2}{dt}=-\mu_{23}\frac{x_3}{L_2}-\frac{R_2}{L_2}x_2+\frac{v_{sc}}{L_2} \tag{9b}$$

$$\frac{dx_3}{dt}=(1-\mu_1)\frac{x_1}{C_{dc}}+\mu_{23}\frac{x_2}{C_{dc}}-\frac{i_o}{C_{dc}} \tag{9c}$$

being x_1 the average value of the current i_{fcf} ($x_1 =< i_{fcf} >$), x_2 is the average value of the SC current ($x_2 =< i_{sc} >$), x_3 is the average value of the dc bus voltage v_{dc} ($x_3 =< v_{dc} >$), μ_1 and μ_{23} are the duty cycle, i.e. average values of the binary control inputs u_1 and u_{23} ($\mu_1 =< u_1 >$, $\mu_{23} =< u_{23} >$), respectively, which take values in [0,1].

Notice that the nonlinear model (9) is a multi-input multi-output (MIMO) system, which can be difficult to control by using classical linear control theory. Now, we are ready to elaborate an appropriate control law that can fulfill all the above mentioned requirements.

IV. Controller Design and Analysis

A. Control objectives

In order to define the control strategy, first one has to establish the control objectives, which can be formulated as following:

i) tight dc bus voltage regulation under load variations,
ii) perfect tracking of SC current i_{sc} to its reference i_{scref},
iii) and asymptotic stability of the whole system.

B. Nonlinear control design

The first control objective is to enforce the dc bus voltage v_{dc} to track a given constant reference signal V_{dcref} [30]. However, it is well known that the boost converter has a non-minimum phase feature ([28], [29]). Such an issue is generally dealt with by resorting an indirect design strategy. More specifically, the objective is to enforce the input inductor current i_{fcf} to track a reference signal, say I_{fcref}. The latter is chosen so that if (in steady state) $i_{fcf}=I_{fcref}$ then $v_{dc}=V_{dcref}$, where $V_{dcref}>v_{fc}$. It follows from power conservation consideration, also called PIPO (Power Input equals Power Output), that I_{fcref} is related to V_{dcref} by the relationship

$$I_{fcref}=\lambda\left(\frac{V_{dcref}i_o-v_{sc}I_{scref}}{v_{fc}}\right) \tag{10}$$

where $\lambda \geq 1$ being an ideality factor introduced to take into account all losses: switching losses in the converters and the losses in the inductances ESR R_1 and R_2.

In order to carry out the first control objective, the following error is introduced

$$e_1=x_1-I_{fcref} \tag{11}$$

Achieving the dc bus voltage regulation objective amounts to enforcing the error e_1 to vanish. To this end, the dynamic of e_1 have to be clearly defined. Deriving (11), it follows from (9a) that:

$$\dot{e}_1=-(1-\mu_1)\frac{x_3}{L_1}-\frac{R_1}{L_1}x_1+\frac{v_{fc}}{L_1}-\dot{I}_{fcref} \tag{12}$$

The goal, now, is to make e_1 exponentially vanishing by enforcing $\dot{e}_1$ to behave as follows

$$\dot{e}_1=-c_1e_1+e_3 \tag{13}$$

where $c_1 > 0$ being a design parameter, and

$$e_3 = x_3 - x_{3d} \tag{14}$$

is the error between the dc bus voltage x_3 and its desired value x_{3d}. The desired value x_{3d} will be specified later.

Combining (12) and (13) the control law of boost converter input signal is obtained,

$$\mu_1 = 1 - \frac{L_1}{x_3}\left\{c_1 e_1 - e_3 + \frac{v_{fc} - R_1 x_1}{L_1} - \dot{I}_{fcref}\right\} \tag{15}$$

In (15) the term e_3 is a damping term introduced in the control law to adjust the output response. Its dynamic will be investigated later.

The next step is to elaborate a control law of buck-boost converter input signal μ_{23}, bearing in mind the second control objective. To this end, the following error is introduced

$$e_2 = x_2 - I_{scref} \tag{16}$$

Its derivative, using (9b), is

$$\dot{e}_2 = -\mu_{23}\frac{x_3}{L_2} - \frac{R_2}{L_2}x_2 + \frac{v_{sc}}{L_2} - \dot{I}_{scref} \tag{17}$$

In order to achieve the tracking objective of the SC current i_{sc}, one can seek that the error e_2 vanish exponentially. This amounts to enforcing its derivative $\dot{e}_2$ to take the following form

$$\dot{e}_2 = -c_2 e_2 \tag{18}$$

where $c_2 > 0$ being a design parameter. Finally, from (16) and (18), the control law μ_{23} can be easily obtained as follows

$$\mu_{23} = \frac{L_2}{x_3}\left\{c_2 e_2 + \frac{v_{sc} - R_2 x_2}{L_2} - \dot{I}_{scref}\right\} \tag{19}$$

Since the two controls laws μ_1 and μ_{23} are clearly defined, the concern is now to check that the stability of the closed loop is perfectly ensured. This will be done in the next subsection.

C. *Stability analysis*

The third control objective can now be analyzed. This can be carried out by checking that the elaborated controllers (15) and (19) stabilize the whole system with the state vector (e_1, e_2, e_3). To this end the following quadratic Lyapunov function is considered

$$V = \frac{1}{2}e_1^2 + \frac{1}{2}e_2^2 + \frac{1}{2}e_3^2 \tag{20}$$

The aim is to make the derivative of V, $\dot{V}$, negative definite. Thus, $\dot{V}$ is obtained from (20) using (13) and (18), which yields to

$$\dot{V} = -c_1 e_1^2 - c_2 e_2^2 + e_3(e_1 + \dot{e}_3) \tag{21}$$

This suggest choosing the derivative $\dot{e}_3$ as follows

$$\dot{e}_3 = -c_3 e_3 - e_1 \tag{22}$$

where $c_3 > 0$ being a design parameter. Indeed, with this choice, the derivative $\dot{V}$ of the Lypunov function can simply rewritten as follows

$$\dot{V} = -c_1 e_1^2 - c_2 e_2^2 - c_3 e_3^2 \tag{23}$$

which means that $\dot{V} \le 0$ and in turn shows that the closed loop system with the state vector (e_1 , e_2 , e_3) is globally asymptotically stable (GAS).

Finally, to achieve the control design one needs the expression of the desired value x_{3d} of dc bus voltage x_3 which is used in the control law (15). Its dynamic can be easily obtained from (22), using (14) and (9c), as follows

$$\dot{x}_{3d} = \frac{1}{C_{dc}}\left[(1-\mu_1)x_1 + \mu_{23}x_2 - i_o\right] + c_3 e_3 + e_1 \tag{24}$$

or equivalently

$$x_{3d} = \frac{1}{s}\left\{\frac{1}{C_{dc}}\left[(1-\mu_1)x_1 + \mu_{23}x_2 - i_o\right] + c_3 e_3 + e_1\right\} \tag{25}$$

where *s* is Laplace operator.

The main results of the paper are now summarized in the following theorem.

Theorem. Consider the closed-loop system consisting of the fuel cell supercapacitor hybrid energy storage system represented by (7a-c), and the controller composed of the control laws (15) and (19). Then, one has:

i) The closed loop system is GAS.
ii) The error e_1 converge to zero implying tight dc bus voltage regulation.
iii) The error e_2 converge to zero implying perfect tracking of SC current i_{sc} to its reference i_{scref}, □

V. SIMULATION RESULTS

The performances of the proposed nonlinear controller are now illustrated by simulation. The controlled system characteristics are listed in Table 1. The PEMFC is with the following characteristics: 262V, 80A, 27kW.

The simulation bench of the hybrid energy storage system control is described by Fig. 5 and is simulated using the MATLAB software. Fig.5 shows the circuit that generates buck-boost converter binary input signals u_2 and u_3 form the control law μ_{23} and i_{scref} according the equations (2) and (8).

The design control parameters are chosen as follows, which proved to be convenient: $c_1 = 10\text{x}10^3$, $c_2 = 2\text{x}10^3$ and $c_3 = 10^2$. The resulting control performances are shown by Figs 5 to 9.

TABLE 2: PARAMETERS OF THE CONTROLLED SYSTEM

Parameter	Value
Inductance L_1 and L_2	3.3mH
Inductances ESR, R_1 and R_2	20mΩ
DC bus Filtering capacitor, C_{dc}	1.66mF
Boost input capacitor, C_{fc}	1.66mF
Supercapapcitor, C_{sc}	21.27F

Supercapacitor ESR, R_{sc}	66mΩ
Switching frequency, f_s	15kHz

Figure 5 and Fig.6 describe the controller performances in presence of a constant reference $I_{scref} = 10A$ and successive load current i_o jumps. The jumps occur between 50A and 20A; and between 20A and 70A. It is seen that the control performances are satisfactory, despite the load current variations. Indeed, Fig.5 shows that the dc voltage v_{dc} is regulated to its desired value $V_{dcref} = 400V$; Fig.6 illustrates the control signals μ_1 and μ_{23} . Figures 7 to 9 describe the controller performances in presence of a constant current load $i_o = 40A$ and successive variations of SC current reference I_{scref} . The variations are performed with jumps between 20A and -30A; and between -30A and 10A. Also, the figures show that the control behavior is satisfactory. Indeed, in Fig. 7 one can shows that the dc voltage v_{dc} is perfectly regulated to its desired value $V_{dcref} = 400V$; Fig.8 illustrates that the SC current i_{sc} tracks its reference signal I_{scref} ; finally, Fig.9 illustrates the control signals μ_1 and μ_{23} .

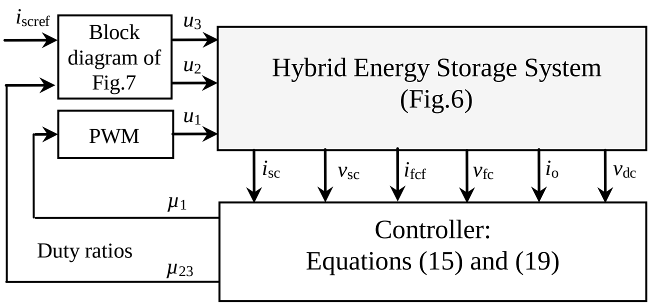

Fig.3: Simulation bench for HESS control

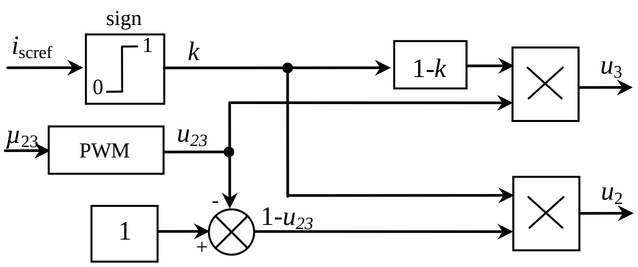

Fig.4: Block diagram of input signals u_2 and u_3 generation

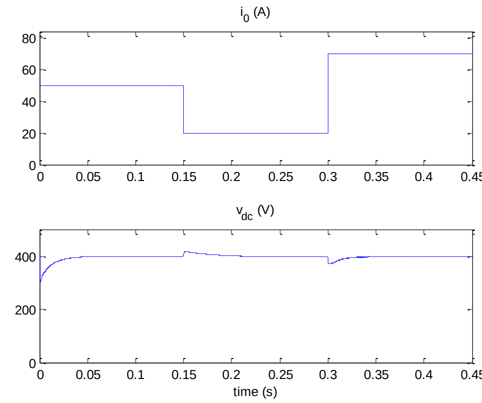

Fig.5: The dc voltage in presence of load current jumps

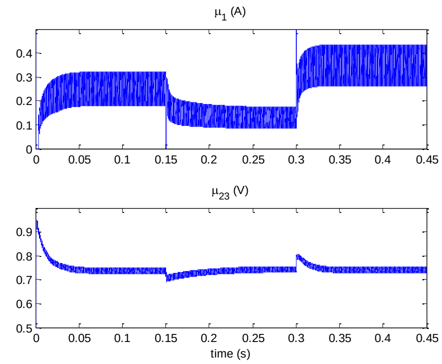

Fig.6: The control signals in presence of load current jumps

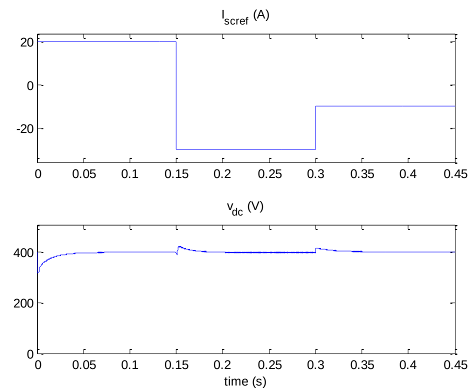

Fig.7: The dc voltage in presence of SC current reference jumps

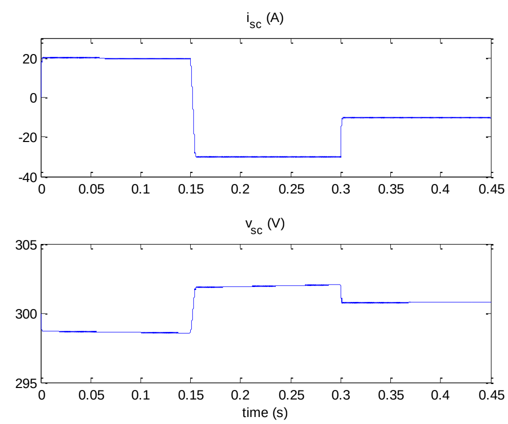

Fig.8: The SC signals in presence of SC current reference jumps

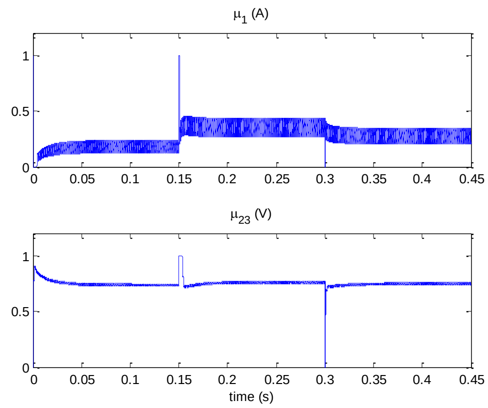

Fig.9: The control signals in presence of SC current reference jumps

VI. Conclusion

The problem of controlling a hybrid energy storage system used in electric vehicle has been considered. The system consists on fuel cell main source and a supercapacitor auxiliary source. In order to manage the energy conversion between sources and load, two dc-dc power converters has been used. The, aim is to elaborate an adequate controller that generates the binary power converters input signals in order to satisfy the following requirements: i) tight dc voltage regulation, ii) perfect tracking of supercapacitor current to its reference and, iii) asymptotic stability of the closed loop system. The controller is obtained from the nonlinear averaged model (9) using a Lyapunov based theory. Using both formal analysis and simulation, it has been proven that the obtained controller achieves the performances for which it was designed.

References

[1] Chan, C.C. "The State of the Art of Electric, Hybrid, and Fuel Cell Vehicles", *In proceedings of the IEEE*, 2007, 95(4), pp.704-718

[2] Momoh, O.D.; Omoigui, M.O "An overview of hybrid electric vehicle technology" *In proc. Of IEEE Vehicle Power and Propulsion Conference, VPPC '09*., Sept. 2009, pp. 1286 – 1292

[3] K. Rajashekara . "Hybrid fuel-cell strategies for clean power generation". *IEEE Transactions on Industry Applications*, 2005, 41, pp.682 – 689,.

[4] J.T. Pukrushpan, H. Peng, and A.G. "Stefanopuolou. Control-oriented modeling and analysis for automotive fuel cell system". *Journal of Dynamic Systems, Measurement, and Control*, 2004, 126, pp.14–25.

[5] J.T. Pukrushpan, A.G. Stefanopoulou, and H. Peng. *Control of Fuel Cell Power Systems: Principles; Modeling; Analysis and Feedback Design*. Springer, 2005.

[6] Guezennec Y, Choi TY, Paganelli G, Rizzoni G. "Supervisory control of fuel cell vehicles and its link to overall system efficiency and low level control requirements. *ACC 2003*; 3(4–6):2055–2061.

[7] C. C. Chan and Y. S. Wong, "Electric vehicles charge forward," *IEEE Power Energy Mag.*, vol. 2, no. 6, Nov./Dec. 2004, pp. 24–33.

[8] Emadi A, Rajashekara K, Williamson SS, Lukic SM. "Topological overview of hybrid electric and fuel cell vehicular power system architectures and configurations". *IEEE Trans. Veh. Technol.* 2005; 54(3), pp.763–70.

[9] Boettner DD, Paganelli G, Guezennec YG, Rizzoni G, Moran MJ. "Proton exchange membrane fuel cell system model for automotive vehicle simulation and control". *J. Energy Resour. Technol.* 2002; 124:20.

[10] Powers WF, Nicastri PR. "Automotive vehicle control challenges in the 21st century". *Control Eng Pract*, 2000; 8(6):605–18.

[11] Emadi A, Ehsani M, Miller JM. *Vehicular electric power systems*. New York: Marcel Dekker Inc.; 2004.

[12] M. B. Burnett and L. J. Borle, "A power system combining batteries and supercapacitors in a solar/hydrogen hybrid electric vehicle," *in Proc. IEEE Conf. Veh. Power Propuls.*, Sep. 7–9, 2005, pp. 711–714.

[13] Khaligh, A.; Zhihao Li. "Battery, Ultracapacitor, Fuel Cell, and Hybrid Energy Storage Systems for Electric, Hybrid Electric, Fuel Cell, and Plug-In Hybrid Electric Vehicles: State of the Art", *IEEE Transactions on Vehicular Technology*, July 2010, 58(6), pp.2806 - 2814

[14] Thounthong, P.; Rael, S.; Davat, B. " Control Strategy of Fuel Cell and Supercapacitors Association for a Distributed Generation System"., *IEEE Trans. On Indus. Elect*.. 54(6), dec. 2007, pp.3225 – 3233.

[15] Alireza P., S. Pierfederici, F. Meibody-Tabar. "Energy control of supercapacitor/fuel cell hybrid power source", *Energy Conversion and Management* , 2008, pp.1637–1644

[16] Marchesoni, M., Vacca, C. "New DC–DC Converter for Energy Storage System Interfacing in Fuel Cell Hybrid Electric Vehicles", *IEEE Trans on Power Elect*., 2007, 22(1), pp.301-308

[17] Samosir, A.S., , Yatim, A.H.M. "Implementation of Dynamic Evolution Control of Bidirectional DC–DC Converter for Interfacing Ultracapacitor Energy Storage to Fuel-Cell System", *IEEE Trans. On Indus. Elect*., 2010, 57(10), pp.3468-3473

[18] Todorovic, M.H.; Palma, L.; Enjeti, P.N. "Design of a Wide Input Range DC–DC Converter With a Robust Power Control Scheme Suitable for Fuel Cell Power Conversion", *IEEE Trans. On Indus. Elect*., 2008, 55(3), pp.1247 - 1255

[19] Rotenberg, D.; Vahidi, A.; Kolmanovsky, I. "Ultracapacitor Assisted Powertrains: Modeling, Control, Sizing, and the Impact on Fuel Economy", *IEEE Trans. On Contr. Syst. Tech*., 2011, 19(3), pp.576 - 589

[20] H. El Fadil, F. Giri, J.M. Guerrero, B. Salhi. "Adaptive Control of Interleaved Boost Converter for Fuel Cell Energy", *In Proc. Of the IEEE American Control Conference*, 2011, pp. 3905-39-10

[21] M. Ortúzar, J. Moreno, and J. Dixon, "Ultracapacitor-based auxiliary energy system for an electric vehicle: Implementation and evaluation," *IEEE Trans. Ind. Electron*., vol. 54, no. 4, pp. 2147–2156, Aug. 2007.

[22] Vahidi, A.; Stefanopoulou, A.; Huei Peng. "Current Management in a Hybrid Fuel Cell Power System: A Model-Predictive Control Approach", *IEEE Trans. On Contr. Syst. Tech*., 2006, 14(6), pp.1047 - 1057

[23] Payman, A.; Pierfederici, S.; Meibody-Tabar, F.; "Energy Management in a Fuel Cell/Supercapacitor Multisource/Multiload Electrical Hybrid System", *IEEE Trans. On Power Elect*., 2009, 24(12), pp.2681 - 2691

[24] Zandi, M.; Payman, A.; Martin, J.-P.; Pierfederici, S.; Davat, B.; Meibody-Tabar, F.; "Energy Management of a Fuel Cell/Supercapacitor/Battery Power Source for Electric Vehicular Applications", *IEEE Trans. On Vehic. Tech*., 2011, 60(2), pp.433 - 443

[25] G. Hoogers. *Fuel Cell Technology Handbook*, CRC Press, 2003.

[26] Nelms RM, Cahela DR, Tatarchuk BJ. "Modeling double-layer capacitor behavior using ladder circuits. *IEEE Trans Aerosp Electron Syst* , 2003; 39(2) pp.430–8.

[27] Spyker RL, Nelms RM. Classical equivalent circuit parameters for a double-layer capacitor. *IEEE Trans Aerosp Electron Syst* , 2000; 36(3), pp. 829–36.

[28] El Fadil, H., Giri, F. "Backstepping basedcontrol of PWM DC–DC boost power converters". *In Proc. of the IEEE Int. Symp. on indust. Elect. (ISIE'07)*, 2007, pp.395–400.

[29] El Fadil, H., Girt, F., Ouadi, H. "Accounting for coils magnetic saturation in controlling DC-DC power converters", *In Proc. of the IEEE Int. Conf. on Contr. Appl. (CCA)*, 2006, pp.3163–3168.

[30] J.-J. E. Slotine and W. Li. *Applied nonlinear control*. Prentice Hall, 1991.